ORIGINAL ARTICLE
See related commentary on pg 1319

Identification of Gene Mutations and Fusion Genes in Patients with Sézary Syndrome

Aparna Prasad[1,2,3,4], Raquel Rabionet[1,2,3,4], Blanca Espinet[4,5], Luis Zapata[1,2,3], Anna Puiggros[4,5], Carme Melero[4,5], Anna Puig[1,2,3,4], Yaris Sarria-Trujillo[1,2,3,4], Stephan Ossowski[1,2], Maria P. Garcia-Muret[6], Teresa Estrach[7], Octavio Servitje[8], Ingrid Lopez-Lerma[9], Fernando Gallardo[4,10], Ramon M. Pujol[4,10] and Xavier Estivill[1,2,3,4,11]

Sézary syndrome is a leukemic form of cutaneous T-cell lymphoma with an aggressive clinical course. The genetic etiology of the disease is poorly understood, with chromosomal abnormalities and mutations in some genes being involved in the disease. The goal of our study was to understand the genetic basis of the disease by looking for driver gene mutations and fusion genes in 15 erythrodermic patients with circulating Sézary cells, 14 of them fulfilling the diagnostic criteria of Sézary syndrome. We have discovered genes that could be involved in the pathogenesis of Sézary syndrome. Some of the genes that are affected by somatic point mutations include *ITPR1*, *ITPR2*, *DSC1*, *RIPK2*, *IL6*, and *RAG2*, with some of them mutated in more than one patient. We observed several somatic copy number variations shared between patients, including deletions and duplications of large segments of chromosome 17. Genes with potential function in the T-cell receptor signaling pathway and tumorigenesis were disrupted in Sézary syndrome patients, for example, *CBLB*, *RASA2*, *BCL7C*, *RAMP3*, *TBRG4*, and *DAD1*. Furthermore, we discovered several fusion events of interest involving *RASA2*, *NFKB2*, *BCR*, *FASN*, *ZEB1*, *TYK2*, and *SGMS1*. Our work has implications for the development of potential therapeutic approaches for this aggressive disease.

Journal of Investigative Dermatology (2016) **136,** 1490−1499; doi:10.1016/j.jid.2016.03.024

INTRODUCTION

Sézary syndrome (SS) is considered the leukemic variant of mycosis fungoides (MF), the most common type of cutaneous T-cell lymphoma (CTCL). SS is classically manifested by the triad of pruritic erythroderma, generalized lymphadenopathy, and the presence of atypical large circulating mononuclear cells with convoluted nuclei (Sézary cells) (Olsen et al., 2011). The prevalence of SS is approximately 0.3 cases per 100,000 people, and it accounts for less than 5% of all CTCLs. SS is observed almost exclusively in adults and elderly patients and is more prevalent in men than women, with a ratio of 2:1. It is an aggressive disease with a poor outcome. (The 5-year overall survival rate is between 30 and 40%). SS may develop de novo or in a patient with a previous diagnosis of MF. The disease generally is much more aggressive, progresses faster, and is more resistant to treatment than classical MF (Agar et al., 2010; Scarisbrick et al., 2015). The genetic etiology of CTCL is largely unknown. Cytogenetic studies of SS have identified abnormalities on chromosomes 1p, 2p, 6q, 9, 10q, 13q, 17p, and 21 (Brito-Babapulle et al., 1997; Espinet et al., 2004; Johnson et al., 1985; Karenko et al., 1997; Limon et al., 1995; Solé et al., 1994).

Next-generation sequencing approaches have revolutionized cancer genomics research with successful application to the study of many hematological cancers, including chronic lymphocytic leukemia (Puente et al., 2011; Quesada et al., 2012), acute myeloid leukemia (Ding et al., 2012; Ley et al., 2008; Mardis et al., 2009), diffuse large B-cell lymphoma (Ngo et al., 2011; Pasqualucci et al., 2011), and Burkitt's lymphoma (Schmitz et al., 2012). Recently, several studies looking at the mutational landscape of CTCL and SS identifying key genomic alterations have been reported (Choi et al., 2015; da Silva Almeida et al., 2015; Kiel et al., 2015; McGirt et al., 2015; Pérez et al., 2015; Ungewickell et al., 2015; Vaque et al., 2014; Wang et al., 2015). Genes involved in T-cell activation and apoptosis, NF-κB signaling, chromatin remodeling, and DNA damage response have been found to be altered (Choi et al., 2015). In addition, signaling pathways including Jak/signal transducer and activator of transcription (STAT) signaling and cell-cycle checkpoint have been shown to be involved in the pathogenesis of CTCL (Pérez et al., 2015; Wang et al., 2015).

[1]Centre for Genomic Regulation (CRG), The Barcelona Institute of Science and Technology, Dr. Aiguader 88, Barcelona 08003, Spain; [2]Universitat Pompeu Fabra (UPF), Barcelona, Spain; [3]CIBER in Epidemiology and Public Health (CIBERESP), Barcelona, Spain; [4]Hospital del Mar Medical Research Institute (IMIM), Barcelona, Spain; [5]Laboratory of Molecular Cytogenetics, Pathology Service, Hospital del Mar, Barcelona, Spain; [6]Dermatology Service, Hospital del Sant Pau, Barcelona, Spain; [7]Department of Dermatology, Hospital Clinic, Barcelona, Spain; [8]Dermatology Service, Hospital de Bellvitge, Barcelona, Spain; [9]Department of Dermatology, Hospital Vall d'Hebron, Barcelona, Spain; [10]Dermatology Service, Hospital del Mar, Barcelona, Spain; and [11]Experimental Genetics, Sidra Medical and Research Centre, Doha, Qatar

Correspondence: Xavier Estivill, Genomics and Disease Group, Bioinformatics and Genomics Program, Centre for Genomic Regulation (CRG), Room 521.01, Dr. Aiguader, 88, 08003 Barcelona, Spain. E-mail: xavier.estivill@crg.eu

Abbreviations: CARD, capsase recruitment domain; CNV, copy number variation; CTCL, cutaneous T-cell lymphoma; kb, kilobase; Mb, megabase; MF, mycosis fungoides; RAG, recombination activating gene; SNV, single nucleotide variant; SS, Sézary syndrome; STAT, signal transducer and activator of transcription

Received 21 December 2015; revised 7 March 2016; accepted 11 March 2016; accepted manuscript published online 30 March 2016; corrected proof published online 24 March 2016

Fusion genes play an important role in tumor development because they might result in disruption of either tumor suppressor genes or activation of proto-oncogenes. Targeting small molecules to these fusion gene products could be crucial in the treatment of cancer. A highly expressed gene fusion between *CTLA4* and *CD28* was discovered in SS in two independent studies (Sekulic et al., 2015; Ungewickell et al., 2015). Here, we have applied whole-exome and RNA sequencing approaches to 15 erythrodermic patients with circulating Sézary cells, 14 of them fulfilling the diagnostic criteria of SS patients, to study the genomic landscape of SS. We have evaluated the somatic mutation spectrum in these samples to identify putative driver mutations in genes involved in the progression of the disease. In addition, we have analyzed their transcriptome to search for fusion genes.

RESULTS AND DISCUSSION

Spectrum of somatic point mutations

We observed a median of 54 somatic point mutations (range, 4–88) in SS patients (Figure 1a and see Supplementary Table S1 online). Two patients (SS06 and SS09) had a relatively low number of somatic point mutations compared with the other patients. One of these (patient SS06) turned out to have a diagnosis of pre-SS. Of all the mutations, 68% of them were C>T transitions (Figure 1b). A higher percentage of C>T transition mutations has also been reported in previous studies involving CTCL, and the possibility of the contribution of UV exposure to MF has been discussed (Choi et al., 2015; McGirt et al., 2015).

We have identified four genes with recurrent somatic mutations in this cohort of SS patients: *TP53*, *ITPR1*, *DSC1*, and *PKHD1L1* (Figure 2). Somatic mutations in *TP53* were found in three patients, including one stop-gain mutation. Recurrent mutations in *TP53* have been reported in patients with CTCL (Choi et al., 2015), SS, and MF (Ungewickell et al., 2015), but recurrent mutations in *ITPR1*, *DSC1*, and *PKHD1L1*, to our knowledge, have not been previously reported in studies of SS. We found damaging somatic mutations in *ITPR1* in two SS patients. A common variant in the gene *ITPR1* has been shown to be associated with susceptibility to breast cancer (Michailidou et al., 2013). *ITPR1* mediates calcium release from the endoplasmic reticulum, and one of the predicted functional partners of *ITPR1* is *BCL2*, which suppresses apoptosis in different cell systems, including lymphohematopoietic and neural cells (Snel et al., 2000; STRING: protein-protein Interaction Networks, 2000). The other gene in which we found highly damaging somatic mutations in two patients was *DSC1*, which has been shown to be associated with different cancer types, including colorectal cancer and liver metastasis (Khan et al., 2006; Schüle et al., 2014). Lastly, somatic mutations in two SS patients were observed in *PKHD1L1*, including one missense and one stop-gain mutation. *PKHD1L1* is a homologue of the autosomal recessive polycystic kidney disease gene, and it encodes a receptor with inducible T-lymphocyte expression, suggesting a role in cellular immunity (Hogan et al., 2003). Somatic mutations in *PKHD1L1* have been implicated in gastric cancer in one study (Liu et al., 2014).

We identified several genes with singleton somatic mutations in our patients, including *PLCG1*, *STAT5B*, *GLI3*, *CARD11*, *NAV3*, *RIPK2*, *IL6*, *RAG2*, and *ITPR2* (see Supplementary Figure S1 online). Some of these genes have been previously shown to be associated with CTCL, including *PLCG1*, *STAT5B*, *GLI3*, *CARD11*, and *NAV3* (Choi et al., 2015; da Silva Almeida et al., 2015; Karenko et al., 2005; Kiel et al., 2015; Ungewickell et al., 2015; Vaque et al., 2014; Wang et al., 2015). We found the same somatic mutation in *PLCG1* (c.1034T>C, S345F) as reported in the study of Vaque et al. (2014) and an N642H mutation in the structurally conserved Src homology 2 (SH2) domain of the *STAT5B* gene (Choi et al., 2015). The oncogenic potential of the N642H mutation in *STAT5B* was shown earlier in pediatric T-cell acute lymphoblastic leukemia (Bandapalli et al., 2014; Kontro et al., 2014), in adult T-cell acute lymphoblastic leukemia (Ma et al., 2015), and in large granular lymphocytic leukemia (Rajala et al., 2013). We observed a somatic missense mutation in *CARD11* and a stop-gain mutation (R792X) in *GLI3* in our dataset. The caspase recruitment domains (CARDs) of the *CARD11* gene are shown to interact with the CARD domain of BCL10, a protein known to function as a positive regulator of cell apoptosis and NF-κB activation (Bertin et al., 2001). *CARD11* is involved in the T-cell receptor signaling pathway, making it a

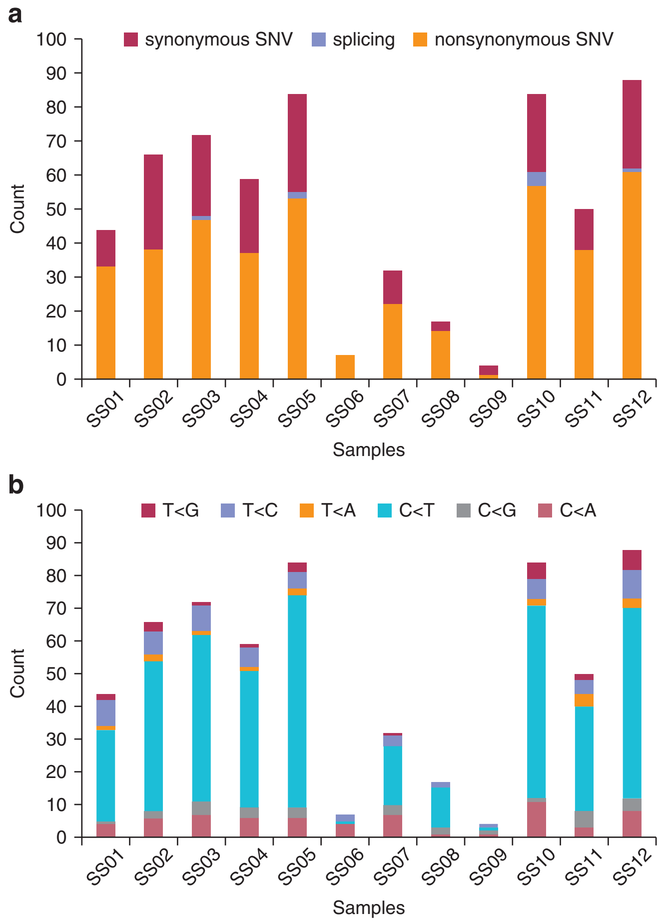

Figure 1. Landscape of somatic point mutations identified in patients with Sézary syndrome. (**a**) Distribution of number of somatic point mutations per sample. This includes somatic synonymous and nonsynonymous mutations and those affecting splice sites. (**b**) Representation of transitions and transversions per sample. A, adenine; C, cytosine; G, guanine; SNV, single nucleotide variation; T, thymine.

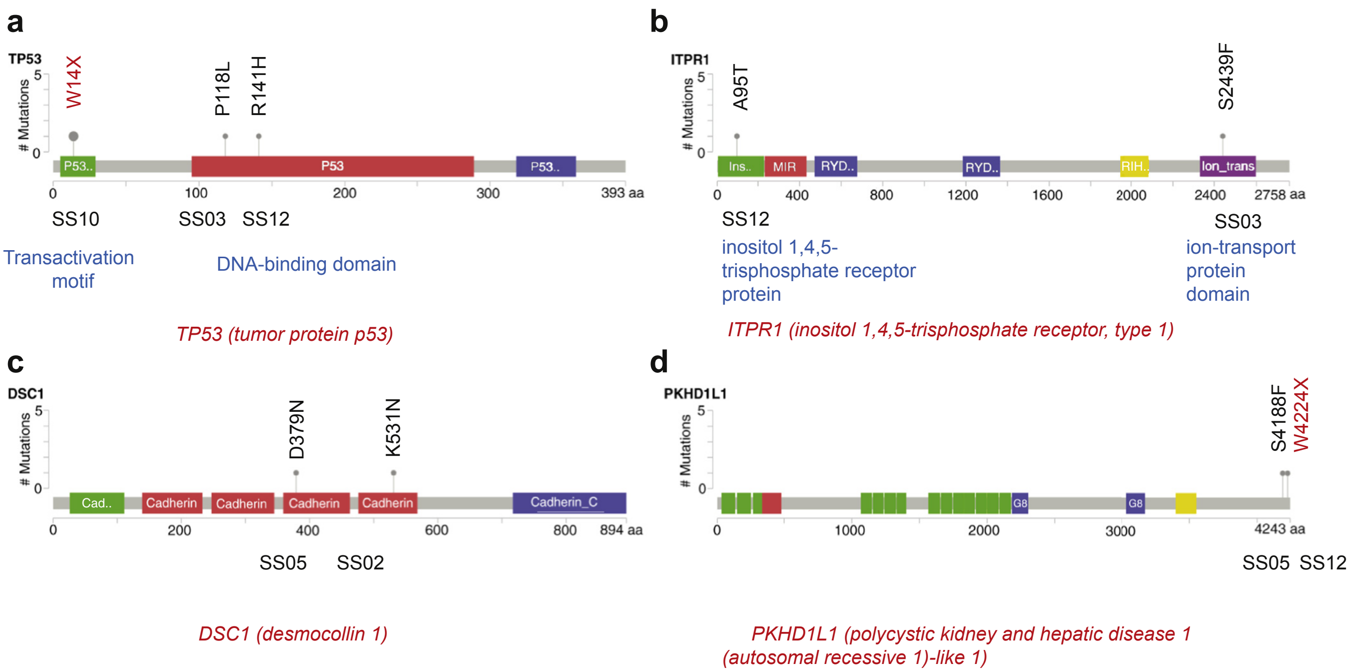

Figure 2. Recurrent somatic mutated genes in patients with Sézary syndrome. The figure schematically represents the location of somatic mutation in the protein structure of each gene. (**a**–**d**) Structure of each gene and samples in which somatic mutations are detected are listed below each mutation. aa, amino acid; Cad, cadherin prodomain like; G8, G8 domain; Ion_trans, ion transport protein; Ins, inositol 1,4,5-trisphosphate/ryanodine receptor; MIR, MIR domain; RYD, RYDR_ITPR pfama, RIH domain; RIH, RyR and IP3R homology associated. The schematic representation of mutations are plotted using the tool MutationMapper from the cBio cancer Genomics Portal (http://cbioportal.org) (Cerami et al., 2012; Gao et al., 2013).

potential candidate gene for SS pathogenesis. We observed a somatic point mutation (Chr12:78569178, G>A) in *NAV3* in one of our SS patients. A previous study identified *NAV3* as a putative tumor suppressor in CTCL, because 50–85% of CTCL patients showed a deletion or translocation affecting *NAV3* (Karenko et al., 2005). However, a later study could not confirm these observations (Marty et al., 2008). These results were also not confirmed with our array comparative genomic hybridization study on tumor stage MF (Salgado et al., 2010). Somatic mutations in *NAV3* have been reported in other cancer types including breast, colorectal, melanoma, and pancreatic carcinomas (Bleeker et al., 2009; Wood et al., 2007). According to the Catalogue of Somatic Mutations in Cancer (i.e., COSMIC), mouse insertional mutagenesis experiments support *NAV3* as a cancer driver gene. To our knowledge, somatic point mutations in *NAV3* have not been reported previously in CTCL studies. NAV3 may have a role in the regulation of IL2 production by T cells and has also been predicted as a high-confidence cancer driver using the IntOGen mutation analysis pipeline (Gonzalez-Perez et al., 2013).

The other genes with singleton somatic point mutations are *IL6*, *RIPK2*, *RAG2*, and *ITPR2*. *IL6* and *RIPK2* are key components of regulation of CD4$^+$ cells and activation/differentiation of alpha-beta T cells involved in immune response. We also observed a somatic missense mutation affecting the plant homeodomain domain of *RAG2* in one SS patient. The plant homeodomain domain is found at the C-terminus of the recombination activating gene (RAG) 2 protein, which modulates its recombination activity (Elkin et al., 2005). This protein was shown to be involved in the process of T-cell differentiation in the thymus, and Choi et al. (2015) reported enrichment of RAG heptamers in CTCL breakpoints. It is important to note that somatic mutations in some genes, including *NAV3* (Chr12:78569178, G>A), *IL6* (Chr7:22767146, G>A), and *ITPR2* (Chr12:26553068, G>A), were detected only using the Agilent SureSelect Target Enrichment Exome (Agilent Technologies, Santa Clara, California, USA) but were missed from the experiments using the Nextera Capture Exome (Illumina, San Diego, California, USA). This was probably not because of different probe coverage between the two capture kits but because the Mutect application was unable to detect these mutations from the Nextera experiments. We used Sanger sequencing to validate these mutations by ruling out false-positive results.

We do not see a similar rate of recurrence for some of the mutations as has been observed in earlier studies, for example, for *PLCG1* and *CARD11*. This is mainly because of the small sample size of our dataset compared with those of other studies (Kiel et al., 2015; Wang et al., 2015). *PLCG1* was first found to be mutated in 9% of the patients with SS (Vaque et al., 2014). In one of the largest studies on SS, the frequency of *PLCG1* mutations was 14% (5 of 37 patients) in the original cohort, and it increased to 21% (14 of 68 patients) in the extension cohort (Wang et al., 2015). Some previous studies have investigated CTCL, which includes patients with both MF and SS. Therefore, both the diagnostic heterogeneity among studies and the clinical heterogeneity of SS per se could contribute to the fact that only some genetic alterations are common between the different studies performed.

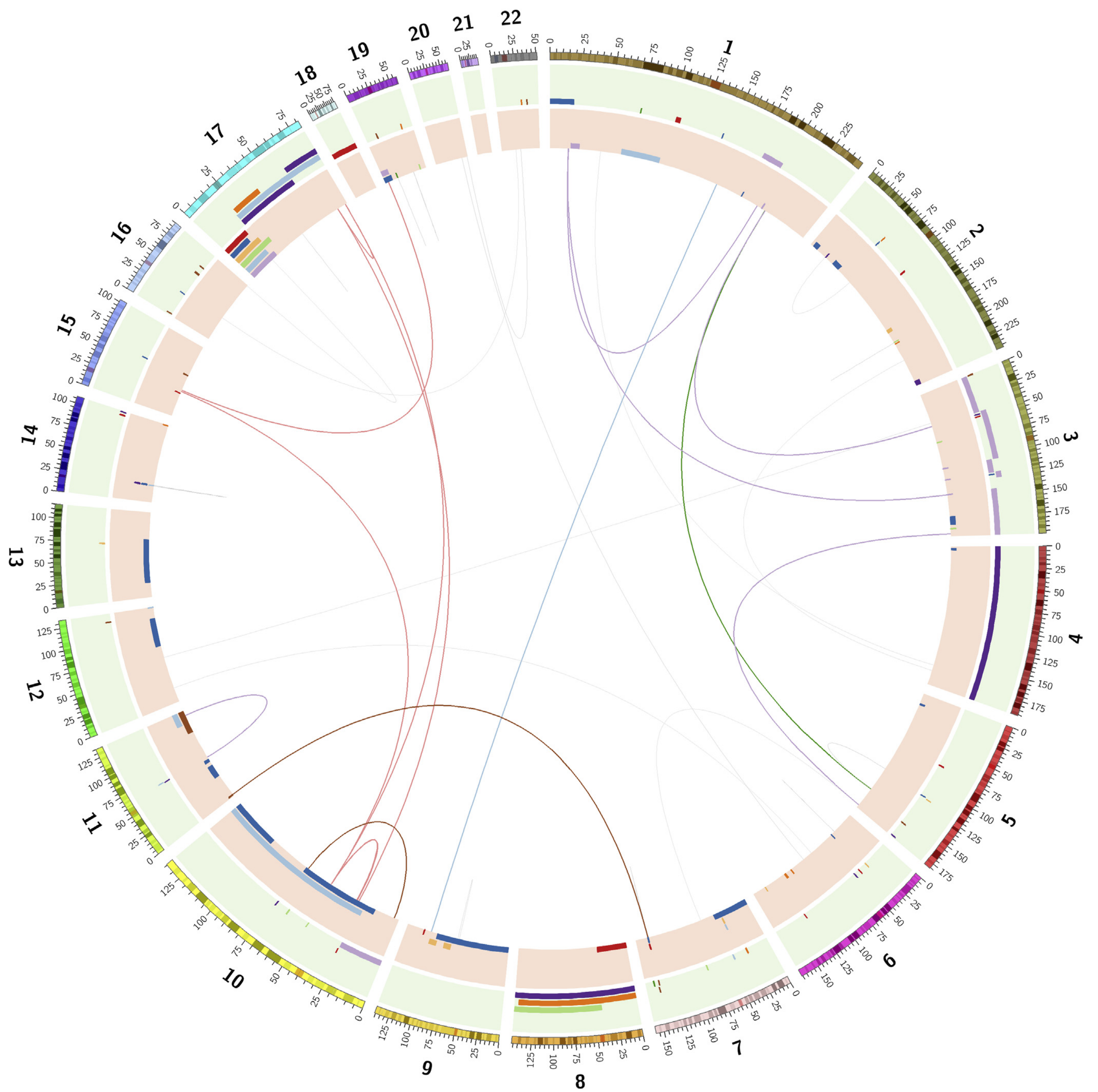

Figure 3. Landscape of somatic copy number variations and fusion events detected in patients with Sézary syndrome. A Circos plot showing a representation of somatic copy number variations and fusion transcripts for 12 Sézary syndrome samples for which DNA sequence data were available. The colored tracks on the rim of the circle represent duplications and deletions. The light green-colored track represents duplications, and the pink colored track represents deletions. The colored lines in the innermost circle show fusion transcripts. This figure is generated using Circos software package (Krzywinski et al., 2009).

Landscape of somatic duplications

We found 61 somatic duplications across 10 patients, with an average of six duplications per patient (see Supplementary Table S2 online and Figure 3). Somatic duplications on chromosome bands 8p23.3−q24.3 (103−146 megabases [Mb]) and 17p11.2−q23.2 (18−21 Mb) were observed in three patients. Among the large-sized duplications (>5 Mb), we observed a somatic duplication of entire chromosome 4, entire chromosome 18, a 26-Mb duplication on 10p15.3−p12.2, and a 19-Mb and a 17-Mb duplication on chromosome 1. Several of the focal somatic duplications (2p15, 3p26.3, 5q23.1, 6p12.3, 7p15.2, 7p12.3−p13, 7q34, 10p12.1, 10q21.3, 12q24.31, 13q21.33, 16p11.2, 16p13.3, 19p13.2, and 19q13.32) encompassed genes that play a role in tumorigenesis or have been found to be involved in several different human cancer types.

We found a 6-kilobase (kb) duplication involving several exons of *ANKRD26* on 10p12.1, encoding a protein containing N-terminal ankyrin repeats, which function in protein-protein interactions. Mutations in this protein are associated with autosomal-dominant thrombocytopenia and myeloid malignancies (Noris et al., 2013). In addition, the

32-kb duplication on chromosome band 16p11.2 involves part of the tumor suppressor *BCL7C* gene (Uehara et al., 2015). Another duplication of interest is 29-kb duplication on chromosome band 6p21.1 that encompasses some exons of *CRIP3*, which is involved in the process of T-cell proliferation. In addition, we observed a 463-kb duplication of chromosome bands 7p12.3−13, encompassing three genes, including *TBRG4* and *RAMP3*. *TBRG4* encodes transforming growth factor-beta regulator 4, and *RAMP3* encodes a protein involved in the G-protein coupled receptor signaling pathway.

Landscape of somatic deletions

A total of 60 somatic deletions were observed across 10 SS samples, with a median of 5 deletions per sample (see Supplementary Table S3 online and Figure 3). Several large deletions (>5 Mb) were shared by patients: a 55−110-Mb deletion on 10p11.1−q26.3 in two patients, a 17-Mb deletion on 11q23.3−q25 in two patients, a 15−25-Mb deletion on 17p12−p13.3 in six patients (encompassing several genes including *TP53*), and a 9-Mb deletion on 19p13.2−p13.3 in two patients.

We observed a somatic deletion of approximately 600 kb on 14q11.2 in patients SS02 and SS07 affecting the *DAD1* gene. The loss of DAD1 protein has been shown to trigger apoptosis (Yulug et al., 1995), and DAD1 protein overexpression is found to be associated with small bowel carcinoid tumors (Kulke et al., 2008). Another interesting example is a 100-kb deletion on 3q23 encompassing several exons of *RASA2* in patient SS01. *RASA2* encodes a proto-oncogene that plays an important role in the mitogen-activated protein kinase signaling pathway that is involved in various cellular functions, including cell proliferation, differentiation, and migration. In the same patient (SS01), we observed another interesting deletion (210 kb) on 3q13.11 encompassing the *CBLB* gene (da Silva Almeida et al., 2015). *CBLB* encodes a proto-oncogene involved in T-cell activation, negative regulation of the T-cell receptor signaling pathway, and negative regulation of alpha-beta T-cell proliferation (Elly et al., 1999). In activated T cells, *CBLB* inhibits *PLCG1* activation and calcium mobilization upon restimulation (Yasuda et al., 2002). The entire chromosome 3 was alternated by duplications and deletions in patient SS01 and was possibly affected by chromothripsis-like rearrangements.

In our patients, chromosome 17 was largely affected by genomic changes, including somatic point mutations and copy number variations. Of special interest is the gene *TP53*, which was affected in 58% of patients (7 of 12), either by somatic point mutations or by somatic deletion with a somatic copy number variation (CNV)/somatic single nucleotide variant (SNV) ratio of 2:1. Although a previous study reported 92.5% of patients with CTCLs (n = 40) with a somatic CNV:SNV ratio of 5.1:1 (Choi et al., 2015), the difference is likely due to the low number of samples (n = 12) in our study on which we have exome sequencing data available. Somatic point mutations in the *TP53* gene were seen in three patients—SS03, SS10, and SS12—whereas large deletions on 17p involving the *TP53* gene were detected in six patients, including SS01, SS02, SS03, SS08, SS10, and SS11. We identified two patients with a double-knockout *TP53* clone. Patient SS03 harbors a 25-Mb deletion on 17p encompassing *TP53* and present in almost all the cells of the patient. This patient also has a subclonal mutation in *TP53*. It is likely that, because of the strong effect of complete loss of functional *TP53*, this clone would be positively selected and, over the course of time, could dominate the tumor population. Patient SS10 has both a stop-gain mutation in *TP53* and a 15-Mb deletion on 17p encompassing *TP53* and is clonal—that is, affecting all the cells—resulting in no functional copy of the *TP53* gene in this patient. These two patients were diagnosed at a relatively early age compared with the rest of the patients, but statistics are insufficient to claim that this is because of the presence of a homozygous loss of *TP53*.

Fusion events

A total of 86 potential fusion events were observed across 10 SS samples (see Supplementary Table S4 online). Fusion RNAs including *TYK2-UPF1*, *COL25A1-NFKB2, FASN-SGMS1*, *SGMS1-ZEB1*, *SPATA21-RASA2*, *PITRM1-HK1*, and *BCR-NDUFAF6* were successfully validated. Complex chromosomal rearrangements were observed in two of our patients (SS04 and SS13), as was evident with the fusion events identified in these patients (see Supplementary Figure S2 online). Patient SS04 had fusion events *FASN-SGMS1* and *SGMS1-ZEB1*. The protein of fatty acid synthase (*FASN*), in some cancer cell lines, gets fused with estrogen receptor-α, in which the N-terminus of fatty acid synthase is fused in-frame with the C-terminus of estrogen receptor-α (Entrez gene, 2008). *FASN* is involved in several cancer types, including hepatocellular carcinoma, colorectal cancer, and prostate cancer (Hao et al., 2014; Madigan et al., 2014; Zaytseva et al., 2014). The other partner of the fusion gene *FASN-SGMS1* is sphingomyelin synthase 1 (*SGMS1*), the activity of which is regulated by the breakpoint cluster region-ABL proto-oncogene, non-receptor tyrosine kinase oncogene. The partner *ZEB1* of the *SGMS1-ZEB1* fusion gene encodes a zinc finger transcription factor and acts as a transcriptional repressor of IL2. The *ZEB1* gene is involved in the process of regulation of T-cell differentiation in the thymus and has been strongly implicated in the pathogenesis of CTCL and SS (Choi et al., 2015; Kiel et al., 2015; McGirt et al., 2015; Wang et al., 2015). Patient SS13 had both *TYK2-UPF1* and *COL25A1- NFKB2* fusion events. The *TYK2* gene was shown to be essential for the differentiation and function of different immune cells, including natural killer cells, B cells, and T-helper cells (Liang et al., 2014). The gene *NFKB2* is a pleiotropic transcription factor that is involved in several pathways including NF-κB signaling, which regulates the transcription of many genes involved in cancer initiation and progression. *NFKB2* was shown to be disrupted in earlier CTCL studies (Choi et al., 2015; Ungewickell et al., 2015), and the effectiveness of using NF-κB inhibitors such as bortezomib has been discussed in a phase II trial (Zinzani et al., 2007). We observed the fusion gene *SPATA21-RASA2* in patient SS01, in whom we also observed the 100-kb somatic deletion on 3q23 encompassing almost all exons of *RASA2*, indicating the mechanism behind formation of this fusion gene. The *PITRM1-HK1* fusion event was found in patient SS05. The elevated level of hexokinase 1 has been shown to promote tumor cells to avoid apoptosis, thereby allowing cell

Table 1. Summary of key genomic changes detected across all 15 patients[1]

	SS01	SS02	SS03	SS04	SS05	SS06	SS07	SS08	SS09	SS10	SS11	SS12	SS13	SS14	SS15
TP53/17p	–	–	X/–					–		X*/–	–	X			
ITPR1			X									X			
DSC1		X			X										
PKHD1L1					X							X*			
PLCG1		X													
STAT5B												X			
GLI3												X*			
CARD11				X											
NAV3	X														
IL6			X												
RIPK2			X												
RAG2				X											
ITPR2			X												
RASA2	–														
CBLB	–														
ALDH1A1		X													
1p21.2–31.3		–													
1q25.3–31.3	+														
1p36.13–36.33										+					
2q37.2–37.3							–								
2q24.1–24.2								–							
Entire chromosome 4							+								
6p21.1 (*CRIP3*)											+				
6q22.31												–			
7p12.3-13 (*TBRG4, RAMP3*)		+													
8p11.1–q24.3			+				+					+			
8p11.21–23.3											–				
9p11.1–q22.32										–					
10p12.1–15.3	+														
10p11.1–q26.3		–								–					
10p12.1 (*ANKRD26*)											+				
11q23.3–25		–			–										
14q11.2 (*DAD1*)		–					–								
16p11.2 (*BCL7C*)										+					
16q21					+										
17p11.1–q25.3		+					+					+			
Entire chromosome 18											+				
19p13.11 (*PDE4C*)						–									
19p13.2–13.3	–									–					
SPATA21-RASA2	ǂ														
FASN-SGMS1				ǂ											
SGMS1-ZEB1				ǂ											
PITRM1-HK1					ǂ										
***ATM* (germline splice mutation)**									Φ						
TYK2-UPF1													ǂ		
COL25A1-NFKB2													ǂ		
chr9:4434675-4434705:*MLLT3*														ǂ	
BCR-NDUFAF6															ǂ

X denotes somatic single nucleotide variant; X* denotes somatic stop-gain single nucleotide variant; + denotes somatic duplication; – denotes somatic deletion; ǂ denotes fusion event; Φ denotes germline splice-site mutation in the *ATM*.

[1]The genes and the genetic alterations that, to the best of our knowledge, have not been reported in previous studies of Sézary syndrome are highlighted in bold. It is important to mention that translocations/deletions in *NAV3* have been reported in an earlier study (Karenko et al., 2005). However, somatic mutations have not been reported in *NAV3* in cutaneous T-cell lymphoma. In addition, somatic mutations in *ATM* have been previously reported. We have not seen studies reporting germline mutations in *ATM* in Sézary syndrome earlier.

proliferation to continue (Azoulay-Zohar et al., 2004). In patient SS15, we observed a fusion gene involving *BCR-NDUFAF6*. A *BCR-ABL* fusion transcript involving exon 8 and exon 4, respectively, has been reported in a SS patient (Callet-Bauchu et al., 2007). Table 1 summarizes the key somatic genomic changes across 15 patients.

In patient SS09, we did not observe any somatic point mutation or copy number variation that could be involved in the pathogenesis of disease in this patient. Although the focus of this study was primarily on somatic mutations, we found a germline splice-site mutation (NM_000051:exon16:c.2377-2A>G) in the *ATM* gene in this patient. The variant has an allele fraction of 0.567, as expected for a heterozygous germline mutation present in all cells of the patient in a diploid locus. This splice-site mutation is affecting the FAT (**F**RAP, **A**TM, **T**RAPP) domain of ATM (ATM serine/threonine kinase). Although the function of this domain is not clear, it has been suggested that the FAT domain interacts with the kinase domain to stabilize the carboxy-terminal end of the protein (Bakkenist and Kastan, 2003). ATM is an important mediator of the DNA damage response pathway. However, in the absence of supporting biological data, we cannot conclude that this particular germline mutation is involved in disease susceptibility in this patient.

Our study presents a complex genomic landscape of SS with several somatic point mutations, copy number variations, and fusion events that could contribute to the pathogenesis of SS. Based on the evidence from our studies and previous studies, it is likely that genes *TP53*, *ITPR1*, *PLCG1*, *CARD11*, *STAT5B*, *RASA2*, *CBLB*, *DAD1*, *TYK2*, *FASN*, *SGMS1*, *NFKB2*, *ZEB1*, *HK1*, and *BCR* could be involved in the pathogenesis of the disease. A number of somatic deletions and duplications identified in this study were shared among patients, indicating that chromosomal instability is a feature of this type of lymphoma. Finally, the fusion genes identified in this study could be targeted for therapeutic implications.

MATERIALS AND METHODS

Sample collection

Fifteen erythrodermic patients presenting with circulation of atypical cerebriform lymphoid cells (Sézary cells) were selected for study. Fourteen patients fulfilled the diagnostic criteria for SS with B2 level of blood involvement proposed by the International Society for Cutaneous Lymphomas (i.e., ISCL) and the European Organization for Research and Treatment of Cancer (i.e., EORTC) (Olsen et al., 2011), and one patient with the de novo erythroderma had less than 1,000 circulating Sézary cells/mm^3 (B1 level of blood involvement) (see Supplementary Table S5 online). B2 level of blood involvement is defined as clonal rearrangement of the T-cell receptor (TCR) in the blood and either 1.0 K/μL or more Sézary cells or one of the 2 criteria outlined by the ISCL, that is, (1) increased CD4$^+$ or CD3$^+$ cells with CD4/CD8 of 10 or more or (2) increase in CD4$^+$cells with an abnormal phenotype ($\geq$ 40% CD4$^+$/CD7$^-$ or $\geq$ 30% CD4$^+$/CD26$^-$) (Vonderheid et al., 2002). Samples came from five different sites in Barcelona: Hospital del Mar, Hospital del Sant Pau, Hospital Clinic, Hospital de Bellvitge, and Hospital Vall d'Hebron. Biological samples from Hospital del Mar were obtained from Parc de Salut MAR Biobank (MARBiobanc). The participation of human subjects in this study was approved by the institutional review board of each hospital, and written informed consent was obtained following Helsinki protocols. Peripheral blood samples were collected for each patient, and CD4$^+$ T lymphocytes were isolated by using magnetic beads (Miltenyi Biotec, Auburn, California, USA). Granulocytes were isolated by dextran sedimentation to obtain matched normal cells. DNA was extracted using the Gentra Puregene Blood Kit (Qiagen, Hilden, Germany). RNA was extracted from matched normal and tumor materials for a total of 10 SS samples using the miRNeasy kit (Qiagen). RNA sequencing was performed on these samples. However exome as well as RNA sequencing data were obtained for only seven of them, as detailed in Supplementary Table S6 online.

Whole-exome sequencing

DNA libraries for 12 matched tumor (CD4$^+$) and normal (granulocyte) cells from SS patients were prepared using the Illumina Nextera DNA Sample Prep kit (Illumina, San Diego, California, USA). The exomes were captured using Nextera rapid capture exome (37 Mb) and sequenced on the Illumina HiSeq 2000 platform as a 100-base pair paired-end run. In addition, genomic DNA from six samples was also captured using the Agilent SureSelect Human All Exon v4 +UTR kit (71 Mb) (Agilent Technologies, Santa Clara, California, USA). The library enriched for target regions was sequenced on the Illumina HiSeq 2000 platform as a 100-base pair paired-end run. The average depth of coverage for the samples captured using the Nextera capture kit was 37× (range = 25−48×), whereas for the samples captured using the Agilent SureSelect capture kit it was 31× (range = 23−49×) of coverage (see Supplementary Table S7 online).

Alignment and SNV calling

The reads generated from the sequencer were aligned to the human genome reference sequence (hg19) using Burrows-Wheeler alignment (BWA-maximal exact match algorithm) (Li and Durbin, 2009). Any duplicate reads were flagged using the MarkDuplicates algorithm from Picard (http://broadinstitute.github.io/picard/). Base quality recalibrations were performed using The Genome Analysis Toolkit haplotype caller (DePristo et al., 2011). Somatic SNVs were detected using MuTect (Cibulskis et al., 2013) and were filtered following the standard recommendation to obtain a set of confident calls. The somatic SNVs obtained using MuTect were further annotated, providing information about the impact of the mutation, the damage potential, and the allele frequency of the somatic SNV in the 1000 Genome (1000 Genomes Project Consortium, 2010) and the Exome Variant Server database (National Heart, Lung, and Blood Institute Exome Sequencing Project, found at http://evs.gs.washington.edu/EVS/). A subset of candidate somatic mutations was validated by Sanger sequencing in CD4$^+$ and granulocyte DNA as control. We analyzed the exome sequencing data for somatic point mutations from both Agilent and Nextera capture kits. For simplification, all the statistics presented in this study are from the Nextera kit, because it was used for all the DNA samples.

Identification of somatic CNVs

Somatic CNVs were identified using an in-house algorithm ClinCNV (manuscript in preparation). ClinCNV computes coverage within samples and across a set of samples and infers CNVs by referring each sample to the computed average and to its matched pair (if available). Further support for CNV is obtained by calculating changes in allele frequency in tumor samples versus matched normal control samples. To define putative deletions and duplications, we established the cutoffs for deletions and duplications at a tumor-to-normal ratio of less than 0.7 and greater than 1.3, respectively, with greater than 77% significant probes in the region. This threshold was relaxed for only one deletion on chromosome 17 in three patients (SS03, SS10, SS11) because the deletion was present in high confidence in three of the other patients, had been reported earlier in literature (Caprini et al., 2009; Vermeer et al., 2008), and was likely to be a true positive. ClinCNV computes the cancer cell fraction for each CNV using an analytical formula published previously (Bassaganyas et al., 2013).

RNA sequencing and fusion transcript discovery

Stranded messenger RNA libraries for 10 tumor ($CD4^+$) samples were generated by polyA selection using the NEBNext Ultra Directional RNA Library Prep Kit for Illumina library preparation kit (New England Biolabs Inc., Ipswich, MA), starting from 700 ng of total RNA. Libraries were sequenced on three lanes of the Illumina Hiseq2500 sequencing platform as a 125-base pair paired-end run. Quality check of the data was performed using FastQC (Babraham Institute, Babraham, Cambridge, United Kingdom; available at http://www.bioinformatics.babraham.ac.uk/projects/fastqc/). The sequencing data for messenger RNA was aligned to the reference genome using STAR (Spliced Transcripts Alignment to Reference), applying parameters optimized for the detection of chimeric reads (Dobin et al., 2013). The resulting potential fusion transcripts were further evaluated both manually and using the R Bioconductor package Chimera (version 1.12.0) (Beccuti et al., 2014). A minimum of 10 supporting (spanning) reads was used as a threshold for fusion transcripts, and the sequence around donor and acceptor sites of potential chimeric reads was manually evaluated to discard potential false positives. We visually inspected Integrated Genome Viewer (Robinson et al., 2011) and RNA expression data and selected some fusion events for validation by real-time PCR.

Accession codes

The exome and RNA sequencing data have been deposited at the European Genome-Phenome Archive (available at http://www.ebi.ac.uk/ega/), which is hosted at the European Bioinformatics institute under accession number EGAS00001001706.

ORCID
Aparna Prasad: http://orcid.org/0000-0002-6786-2313

CONFLICT OF INTEREST
The authors state no conflict of interest.

ACKNOWLEDGMENTS
This project was funded by "Retos de la Sociedad 2013: Europa Redes y Gestores" Programme from the Spanish Ministry of Economy and Competitiveness no. SAF2013-49108-R (to XE) and RD12/0036/0044 Red Temática de Investigación Cooperativa en Cáncer, Fondo Europeo de Desarrollo Regional (to BE, FG, and RP), the Generalitat de Catalunya AGAUR 2014 SGR-1138 (to XE) and 2014 SGR-585 (to BE, A Puiggros, and FG), the European Commission 7th Framework Program (FP7/2007-2013) under grant agreement 282510 (A BLUEPRINT of haematopoietic Epigenomes to XE) and 262055 (European Sequencing and Genotyping Infrastructure to XE), Instituto de Salud Carlos III FEDER (PT13/0010/0005), and the "Xarxa de Bancs de tumors sponsored by Pla Director d'Oncologia de Catalunya." We would also like to thank "Xarxa de Limfomes Cutanis de Catalunaya." A Prasad is a Marie Curie Postdoctoral fellow supported by the European Commission 7th framework program (FP7/2007-2013) under grant agreement no. 625356. We acknowledge the support of the Spanish Ministry of Economy and Competitiveness, Centro de Excelencia Severo Ochoa 2013-2017, SEV-2012-0208.

SUPPLEMENTARY MATERIAL
Supplementary material is linked to the online version of the paper at www.jidonline.org, and at http://dx.doi.org/10.1016/j.jid.2016.03.024.

REFERENCES

1000 Genomes Project Consortium. A map of human genome variation from population-scale sequencing. Nature 2010;467:1061–73.

Agar NS, Wedgeworth E, Crichton S, Mitchell TJ, Cox M, Ferreira S, et al. Survival outcomes and prognostic factors in mycosis fungoides/Sezary syndrome: validation of the revised International Society for Cutaneous Lymphomas/European Organisation for Research and Treatment of Cancer staging proposal. J Clin Oncol 2010;28:4730–9.

Azoulay-Zohar H, Israelson A, Abu-Hamad S, Shoshan-Barmatz V. In self-defence: hexokinase promotes voltage-dependent anion channel closure and prevents mitochondria-mediated apoptotic cell death. Biochem J 2004;377:347–55.

Bakkenist C, Kastan M. DNA damage activates ATM through intermolecular autophosphorylation and dimer dissociation. Nature 2003;421:499–506.

Bandapalli OR, Schuessele S, Kunz JB, Rausch T, Stütz AM, Tal N, et al. The activating STAT5B N642H mutation is a common abnormality in pediatric T-cell acute lymphoblastic leukemia and confers a higher risk of relapse. Haematologica 2014;99:e188–92.

Bassaganyas L, Bea S, Escaramis G, Tornador C, Salaverria I, Zapata L, et al. Sporadic and reversible chromothripsis in chronic lymphocytic leukemia revealed by longitudinal genomic analysis. Leukemia 2013;27:2376–9.

Beccuti M, Carrara M, Cordero F, Lazzarato F, Donatelli S, Nadalin F, et al. Chimera: a bioconductor package for secondary analysis of fusion products. Bioinformatics 2014;30:3556–7.

Bertin J, Wang L, Guo Y, Jacobson M, Poyet J, Srinivasula S, et al. CARD11 and CARD14 are novel caspase recruitment domain (CARD)/membrane-associated guanylate kinase (MAGUK) family members that interact with BCL10 and activate NF-kappa B. J Biol Chem 2001;276:11877–82.

Bleeker FE, Lamba S, Rodolfo M, Scarpa A, Leenstra S, Vandertop WP, et al. Mutational profiling of cancer candidate genes in glioblastoma, melanoma and pancreatic carcinoma reveals a snapshot of their genomic landscapes. Hum Mutat 2009;30:E451–9.

Brito-Babapulle V, Maljaie SH, Matutes E, Hedges M, Yuille M, Catovsky D. Relationship of T leukaemias with cerebriform nuclei to T-prolymphocytic leukaemia: a cytogenetic analysis with in situ hybridization. Br J Haematol 1997;96:724–32.

Callet-Bauchu E, Salles G, Gazzo S, Dalle S, Berger F, Hayette S. Identification of a novel e8/a4 BCR/ABL fusion transcript in a case of a transformed Sezary syndrome. Haematologica 2007;92:1277–8.

Caprini E, Cristofoletti C, Arcelli D, Fadda P, Citterich M, Sampogna F, et al. Identification of key regions and genes important in the pathogenesis of Sezary syndrome by combining genomic and expression microarrays. Cancer Res 2009;69:8438–46.

Cerami E, Gao J, Dogrusoz U, Gross BE, Sumer SO, Aksoy BA, et al. The cBio cancer genomics portal: an open platform for exploring multidimensional cancer genomics data. Cancer Discov 2012;2:401–4.

Choi J, Goh G, Walradt T, Hong BS, Bunick CG, Chen K, et al. Genomic landscape of cutaneous T cell lymphoma. Nat Genet 2015;47:1011–9.

Cibulskis K, Lawrence MS, Carter SL, Sivachenko A, Jaffe D, Sougnez C, et al. Sensitive detection of somatic point mutations in impure and heterogeneous cancer samples. Nat Biotechnol 2013;31:213–9.

da Silva Almeida AC, Abate F, Khiabanian H, Martinez-Escala E, Guitart J, Tensen CP, et al. The mutational landscape of cutaneous T cell lymphoma and Sézary syndrome. Nat Genet 2015;47:1465–70.

DePristo MA, Banks E, Poplin R, Garimella KV, Maguire JR, Hartl C, et al. A framework for variation discovery and genotyping using next-generation DNA sequencing data. Nat Genet 2011;43:491–8.

Ding L, Ley TJ, Larson DE, Miller CA, Koboldt DC, Welch JS, et al. Clonal evolution in relapsed acute myeloid leukaemia revealed by whole-genome sequencing. Nature 2012;481:506–10.

Dobin A, Davis CA, Schlesinger F, Drenkow J, Zaleski C, Jha S, et al. STAR: ultrafast universal RNA-seq aligner. Bioinformatics 2013;29:15–21.

Elkin SK, Ivanov D, Ewalt M, Ferguson CG, Hyberts SG, Sun ZY, et al. A PHD finger motif in the C terminus of RAG2 modulates recombination activity. J Biol Chem 2005;280:28701–10.

Elly C, Witte S, Zhang Z, Rosnet O, Lipkowitz S, Altman A, et al. Tyrosine phosphorylation and complex formation of Cbl-b upon T cell receptor stimulation. Oncogene 1999;18:1147–56.

Entrez gene. https://www.ncbi.nlm.nih.gov/gene/2194; 2008 (accessed October 2015).

Espinet B, Salido M, Pujol R, Florensa L, Gallardo F, Domingo A, et al. Genetic characterization of Sezary's syndrome by conventional cytogenetics and cross-species color banding fluorescent in situ hybridization. Haematologica 2004;89:165–73.

Gao J, Aksoy BA, Dogrusoz U, Dresdner G, Gross B, Sumer SO, et al. Integrative analysis of complex cancer genomics and clinical profiles using the cBIoPortal. Sci Signal 2013;6:pl1.

Gonzalez-Perez A, Perez-Llamas C, Deu-Pons J, Tamborero D, Schroeder MP, Jene-Sanz A, et al. IntOGen-mutations identifies cancer drivers across tumor types. Nat Methods 2013;10:1081–2.

Hao Q, Li T, Zhang X, Gao P, Qiao P, Li S, et al. Expression and roles of fatty acid synthase in hepatocellular carcinoma. Oncol Rep 2014;32:2471–6.

Hogan MC, Griffin MD, Rossetti S, Torres VE, Ward CJ, Harris PC. PKHDL1, a homolog of the autosomal recessive polycystic kidney disease gene, encodes a receptor with inducible T lymphocyte expression. Hum Mol Genet 2003;12:685–98.

Johnson GA, Dewald GW, Strand WR, Winkelmann RK. Chromosome studies in 17 patients with the Sézary syndrome. Cancer 1985;55:2426–33.

Karenko L, Hahtola S, Paivinen S, Karhu R, Syrja S, Kahkonen M, et al. Primary cutaneous T-cell lymphomas show a deletion or translocation affecting NAV3, the human UNC-53 homologue. Cancer Res 2005;65:8101–10.

Karenko L, Hyytinen E, Sarna S, Ranki A. Chromosomal abnormalities in cutaneous T-cell lymphoma and in its premalignant conditions as detected by G-banding and interphase cytogenetic methods. J Invest Dermatol 1997;108:22–9.

Khan K, Hardy R, Haq A, Ogunbiyi O, Morton D, Chidgey M. Desmocollin switching in colorectal cancer. Br J Cancer 2006;95:1367–70.

Kiel M, Sahasrabuddhe A, Rolland D, Velusamy T, Chung F, Schaller M, et al. Genomic analyses reveal recurrent mutations in epigenetic modifiers and the JAK-STAT pathway in Sezary syndrome. Nat Comm 2015;6:8470.

Kontro M, Kuusanmäki H, Eldfors S, Burmeister T, Andersson EI, Bruserud O, et al. Novel activating STAT5B mutations as putative drivers of T-cell acute lymphoblastic leukemia. Leukemia 2014;28:1738–42.

Krzywinski M, Schein J, Birol I, Connors J, Gascoyne R, Horsman D, et al. Circos: an information aesthetic for comparative genomics. Genome Res 2009;19:1639–45.

Kulke MH, Freed E, Chiang DY, Philips J, Zahrieh D, Glickman JN, et al. High-resolution analysis of genetic alterations in small bowel carcinoid tumors reveals areas of recurrent amplification and loss. Genes Chromosom Cancer 2008;47:591–603.

Ley TJ, Mardis ER, Ding L, Fulton B, McLellan MD, Chen K, et al. DNA sequencing of a cytogenetically normal acute myeloid leukaemia genome. Nature 2008;456:66–72.

Li H, Durbin R. Fast and accurate short read alignment with Burrows-Wheeler transform. Bioinformatics 2009;25:1754–60.

Liang Y, Zhu Y, Xia Y, Peng H, Yang XK, Liu YY, et al. Therapeutic potential of tyrosine kinase 2 in autoimmunity. Expert Opin Ther Targets 2014;18:571–80.

Limon J, Nedoszytko B, Brozek I, Hellmann A, Zajaczek S, Lubiński J, et al. Chromosome aberrations, spontaneous SCE, and growth kinetics in PHA-stimulated lymphocytes of five cases with Sézary syndrome. Cancer Genet Cytogenet 1995;83:75–81.

Liu J, McCleland M, Stawiski EW, Gnad F, Mayba O, Haverty PM, et al. Integrated exome and transcriptome sequencing reveals ZAK isoform usage in gastric cancer. Nat Commun 2014;5:3830.

Ma X, Wen L, Wu L, Wang Q, Yao H, Ma L, et al. Rare occurrence of a STAT5B N642H mutation in adult T-cell acute lymphoblastic leukemia. Cancer Genet 2015;208:52–3.

Madigan AA, Rycyna KJ, Parwani AV, Datiri YJ, Basudan AM, Sobek KM, et al. Novel nuclear localization of fatty acid synthase correlates with prostate cancer aggressiveness. Am J Pathol 2014;184:2156–62.

Mardis ER, Ding L, Dooling DJ, Larson DE, McLellan MD, Chen K, et al. Recurring mutations found by sequencing an acute myeloid leukemia genome. N Engl J Med 2009;361:1058–66.

Marty M, Prochazkova M, Laharanne E, Chevret E, Longy M, Jouary T, et al. Primary cutaneous T-cell lymphomas do not show specific NAV3 gene deletion or translocation. J Invest Dermatol 2008;128:2458–66.

McGirt LY, Jia P, Baerenwald DA, Duszynski RJ, Dahlman KB, Zic JA, et al. Whole-genome sequencing reveals oncogenic mutations in mycosis fungoides. Blood 2015;126:508–19.

Michailidou K, Hall P, Gonzalez-Neira A, Ghoussaini M, Dennis J, Milne RL, et al. Large-scale genotyping identifies 41 new loci associated with breast cancer risk. Nat Genet 2013;45:353–61, 61e1–2.

Ngo VN, Young RM, Schmitz R, Jhavar S, Xiao W, Lim KH, et al. Oncogenically active MYD88 mutations in human lymphoma. Nature 2011;470:115–9.

Noris P, Favier R, Alessi MC, Geddis AE, Kunishima S, Heller PG, et al. ANKRD26-related thrombocytopenia and myeloid malignancies. Blood 2013;122:1987–9.

Olsen E, Whittaker S, Kim Y, Duvic M, Prince H, Lessin S, et al. Clinical end points and response criteria in mycosis fungoides and Sezary syndrome: a consensus statement of the International Society for Cutaneous Lymphomas, the United States Cutaneous Lymphoma Consortium, and the Cutaneous Lymphoma Task Force of the European Organisation for Research and Treatment of Cancer. J Clin Oncol 2011;29:2598–607.

Pasqualucci L, Trifonov V, Fabbri G, Ma J, Rossi D, Chiarenza A, et al. Analysis of the coding genome of diffuse large B-cell lymphoma. Nat Genet 2011;43:830–7.

Pérez C, González-Rincón J, Onaindia A, Almaráz C, García-Díaz N, Pisonero H, et al. Mutated JAK kinases and deregulated STAT activity are potential therapeutic targets in cutaneous T-cell lymphoma. Haematologica 2015;100:e450–3.

Puente XS, Pinyol M, Quesada V, Conde L, Ordóñez GR, Villamor N, et al. Whole-genome sequencing identifies recurrent mutations in chronic lymphocytic leukaemia. Nature 2011;475:101–5.

Quesada V, Conde L, Villamor N, Ordóñez GR, Jares P, Bassaganyas L, et al. Exome sequencing identifies recurrent mutations of the splicing factor SF3B1 gene in chronic lymphocytic leukemia. Nat Genet 2012;44:47–52.

Rajala HL, Eldfors S, Kuusanmäki H, van Adrichem AJ, Olson T, Lagström S, et al. Discovery of somatic STAT5b mutations in large granular lymphocytic leukemia. Blood 2013;121:4541–50.

Robinson JT, Thorvaldsdottir H, Winckler W, Guttman M, Lander ES, Getz G, et al. Integrative genomics viewer. Nat Biotechnol 2011;29:24–6.

Salgado R, Servitje O, Gallardo F, Vermeer MH, Ortiz-Romero PL, Karpova MB, et al. Oligonucleotide array-CGH identifies genomic subgroups and prognostic markers for tumor stage mycosis fungoides. J Invest Dermatol 2010;130:1126–35.

Scarisbrick JJ, Prince HM, Vermeer MH, Quaglino P, Horwitz S, Porcu P, et al. Cutaneous Lymphoma International Consortium study of outcome in advanced stages of mycosis fungoides and Sézary syndrome: effect of specific prognostic markers on survival and development of a prognostic model. J Clin Oncol 2015;33:3766–73.

Schmitz R, Young RM, Ceribelli M, Jhavar S, Xiao W, Zhang M, et al. Burkitt lymphoma pathogenesis and therapeutic targets from structural and functional genomics. Nature 2012;490:116–20.

Schüle S, Neuhäuser C, Rauchfuß F, Knösel T, Settmacher U, Altendorf-Hofmann A. The influence of desmocollin 1-3 expression on prognosis after curative resection of colorectal liver metastases. Int J Colorectal Dis 2014;29:9–14.

Sekulic A, Liang WS, Tembe W, Izatt T, Kruglyak S, Kiefer JA, et al. Personalized treatment of Sézary syndrome by targeting a novel CTLA4:CD28 fusion. Mol Genet Genomic Med 2015;3:130–6.

Snel B, Lehmann G, Bork P, Huynen MA. STRING: a web-server to retrieve and display the repeatedly occurring neighbourhood of a gene. Nucleic Acids Res 2000;28:3442–4.

Solé F, Woessner S, Vallespi T, Pérez Losada A, Florensa L, Irriguible D, et al. Cytogenetic studies in five patients with Sézary syndrome. Cancer Genet Cytogenet 1994;75:130–2.

STRING: protein-protein Interaction Networks. http://string-db.org; 2000 (accessed October 2015).

Uehara T, Kage-Nakadai E, Yoshina S, Imae R, Mitani S. The tumor suppressor BCL7B functions in the Wnt signaling pathway. PLoS Genet 2015;11:e1004921.

Ungewickell A, Bhaduri A, Rios E, Reuter J, Lee CS, Mah A, et al. Genomic analysis of mycosis fungoides and Sézary syndrome identifies recurrent alterations in TNFR2. Nat Genet 2015;47:1056–60.

Vaque J, Gomez-Lopez G, Monsalvez V, Varela I, Martinez N, Perez C, et al. PLCG1 mutations in cutaneous T-cell lymphomas. Blood 2014;123:2034–43.

Vermeer MH, van Doorn R, Dijkman R, Mao X, Whittaker S, van Voorst Vader PC, et al. Novel and highly recurrent chromosomal alterations in Sézary syndrome. Cancer Res 2008;68:2689−98.

Vonderheid EC, Bernengo MG, Burg G, Duvic M, Heald P, Laroche L, et al. Update on erythrodermic cutaneous T-cell lymphoma: report of the International Society for Cutaneous Lymphomas. J Am Acad Dermatol 2002;46:95−106.

Wang L, Ni X, Covington KR, Yang BY, Shiu J, Zhang X, et al. Genomic profiling of Sézary syndrome identifies alterations of key T cell signaling and differentiation genes. Nat Genet 2015;47:1426−34.

Wood LD, Parsons DW, Jones S, Lin J, Sjöblom T, Leary RJ, et al. The genomic landscapes of human breast and colorectal cancers. Science 2007;318:1108−13.

Yasuda T, Tezuka T, Maeda A, Inazu T, Yamanashi Y, Gu H, et al. Cbl-b positively regulates Btk-mediated activation of phospholipase C-gamma2 in B cells. J Exp Med 2002;196:51−63.

Yulug IG, See CG, Fisher EM, Ylug IG. The DAD1 protein, whose defect causes apoptotic cell death, maps to human chromosome 14. Genomics 1995;26:433−5.

Zaytseva YY, Elliott VA, Rychahou P, Mustain WC, Kim JT, Valentino J, et al. Cancer cell-associated fatty acid synthase activates endothelial cells and promotes angiogenesis in colorectal cancer. Carcinogenesis 2014;35:1341−51.

Zinzani P, Musuraca G, Tani M, Stefoni V, Marchi E, Fina M, et al. Phase II trial of proteasome inhibitor bortezomib in patients with relapsed or refractory cutaneous T-cell lymphoma. J Clin Oncol 2007;25:4293−7.